Available online at www.sciencedirect.com
SCIENCE DIRECT
Trans. Nonferrous Met. Soc. China 16(2006) 467−472
Transactions of Nonferrous Metals Society of China
www.csu.edu.cn/ysxb/

Preparation and property of spinel $LiMn_2O_4$ material by co-doping anti-electricity ions

XIAO Jin(肖 劲), ZHU Hua-li(朱华丽), CHEN Zhao-yong(陈召勇),
PENG Zhong-dong(彭忠东), HU Guo-rong(胡国荣)

School of Metallurgical Science and Engineering, Central South University, Changsha 410083, China

Received 20 June 2005; accepted 8 September 2005

Abstract: $LiMn_{2-x}M_xO_{4-y}F_y$(x=0.05; y=0.05; M=Al, Co, Cr and Mg, separately), as the cathode material, was synthesized by the method of high temperature solid-state reaction in laboratory. The results of charge-discharge test show that the properties of $LiMn_{1.95}M_{0.05}O_{3.95}F_{0.05}$(M= Al, Mg) are obviously superior to those of $LiMn_2O_4$. Through the condition experiments on sintering temperature, it is found that the materials present the integrate crystal structure and favorable cycle performance at 800 ℃. The research on the effects of different Mg^{2+} sources on the properties of $LiMn_{2-x}Mg_xO_{4-y}F_y$ shows that, with $Mg(OH)_2$ and LiF as the reagents respectively offering Mg^{2+} and F^-, $LiMn_{1.95}Mg_{0.05}O_{3.95}F_{0.05}$ synthesized has integrate crystal structure and its capacity hardly fades. The results of cyclic voltammetry indicate that the shape of two couples of redox peaks of the material synthesized by co-doping anti-electricity ions is more integrate and symmetrical than that of pure spinel $LiMn_2O_4$, which reveals that the co-doping material possesses preferable electrochemical reversibility.

Key words: Li-ion batteries; cathode material; $LiMn_2O_4$; Co-doping; anti-electricity ions; cycle performance

1 Introduction

At present, $LiCoO_2$ is almost the only cathode material of Li-ion batteries, which can be used in large-scale commercialization, because such material possesses high specific capacity, ease of preparation, high discharging flat and favorable cycle performance. However, cobalt, as the primary raw material, hinders the development of Li-ion batteries due to its high cost and toxicity[1]. Therefore searching for new materials which can overcome the disadvantages above has received a great deal of attention. The cathode materials of Li-ion batteries are presently $LiCoO_2$, $LiNiO_2$, $LiMnO_2$ and $LiVO_2$ with layered structure and their ramifications, spinel $LiMn_2O_4$ and olivine $LiFePO_4$, etc[2−10]. As for the research on spinel $LiMn_2O_4$, its advantages, such as ease of preparation, wide range of raw materials, low cost, charge-discharge with high-current and well security, especially its environment-friendliness, have been acknowledged in academia. But its disadvantages, namely low specific capacity, rapid capacity-fading, poor cyclic efficiency and severe local action, etc, block its industrialization. In the past ten years, researchers have been trying to improve the properties of $LiMn_2O_4$ by reducing the Jahn-Teller effect and avoiding dissolved loss of Mn, etc[11,12]. Moreover, many people are searching for the inert electrolyte system of new style which can be fitted for the cathode material of $LiMn_2O_4$ which namely possesses indissolubility in such system[13].

The research indicated that the cathode material of $LiMn_2O_4$ doped with some certain metal ions had better cycle performance, and yet the specific capacity of this cathode material was reduced. While some anions, such as F^-, when doped into such material, could enhance its specific capacity, but could hardly improve the cycle performance[14,15]. In this paper, the author selected metal ions combined with the anion of F^- as anti-electricity ions co-doped into the spinel $LiMn_2O_4$ material to not only enhance its specific capacity, but improve the cycle performance.

2 Experimental

2.1 Choice for doped ions

Corresponding author: XIAO Jin; Tel: +86-731-8876454; E-mail: 13607445108@hnmcc.com

There are many choices for metal ions doped into the spinel $LiMn_2O_4$ material. The appropriate ions were selected from the following four aspects: 1) the stability of such ions; 2) the stability of the oxides of such ions; 3) the intensity of M-O bonds; 4) the radius of such ions. Through the comprehensive consideration, four metal ions, Co^{3+}, Cr^{3+}, Al^{3+} and Mg^{2+} were selected, and the anion of F^- was as the anti-electricity ions co-doped into the spinel $LiMn_2O_4$ material. The structural parameters of some ions are listed in Table 1.

2.2 Preparation of $LiMn_2O_4$ material co-doped with anti-electricity ions

The $LiMn_2O_4$ material co-doped with anti-electricity ions was synthesized by the method of conventional high temperature solid-state reaction. The experiment was done with utilizing electrolyzed MnO_2 (EMD) and Li_2CO_3 as the raw materials, and LiF and MgF_2 as the reagents offering F, and $Al(OH)_3$, Co_3O_4, Cr_2O_3, $Mg(OH)_2$ and MgF_2 as the reagents offering Al^{3+}, Co^{3+}, Cr^{3+} and Mg^{2+} separately, to synthesize $LiMn_{2-x}M_xO_{4-y}F_y$ (x=0.05; y=0.05; M= Al, Co, Cr and Mg).

3 Results and discussion

3.1 Charge-discharge studies

The first charge-discharge capacity, the first coulomb efficiency, the data of reversible capacity and the efficiency of capacity retaining of $LiMn_{2-x}M_xO_{4-y}F_y$ (x=0.05; y=0.05; M= Al, Co, Cr, Mg) co-doped with anti-electricity ions during prior 20 times charge-discharge process are listed in Table 2, where the data of the first cycle process show that the first reversible capacity is relatively changed. The first reversible capacity of both $LiMn_{1.95}Al_{0.05}O_{3.95}F_{0.05}$ and $LiMn_{1.95}Cr_{0.05}O_{3.95}F_{0.05}$ are higher than that of pure-phase $LiMn_2O_4$ and lower than that of $LiMn_2O_{3.95}F_{0.05}$, while capacities of $LiMn_{1.95}Co_{0.05}O_{3.95}F_{0.05}$ and $LiMn_{1.95}Mg_{0.05}O_{3.95}F_{0.05}$ are both lower than those of pure-phase $LiMn_2O_4$ and $LiMn_2O_{3.95}F_{0.05}$. In addition, the first coulomb efficiencies of the materials co-doped is also changed. The first coulomb efficiency of materials co-doped with Al, Cr, Mg and F is considerably enhanced, especially that of $LiMn_{2-x}Mg_xO_{4-y}F_y$ up to 97.2%.

Fig.1 depicts the cycle performance curves of the doping materials during prior 20 times charge-discharge process. It can be seen from Table 2 and Fig.1, that reversible capacities and the efficiencies of capacity retaining of $LiMn_{1.95}Al_{0.05}O_{3.95}F_{0.05}$ and $LiMn_{1.95}Mg_{0.05}O_{3.95}F_{0.05}$ during the prior 20 times charge-discharge process are superior to those of other materials. Compared with $LiMn_{1.95}Mg_{0.05}O_{3.95}F_{0.05}$, the first capacity of $LiMn_{1.95}Al_{0.05}O_{3.95}F_{0.05}$ is 5.88 mA·h/g higher, and yet such data (118.07 mA·h/g and 117.57 mA·h/g) of these two materials are closed after 20 times charge-discharge. Moreover, the efficiencies of capacity retaining of $LiMn_{1.95}Al_{0.05}O_{3.95}F_{0.05}$ and $LiMn_{1.95}Mg_{0.05}$-

Table 1 Structural parameters of some ions

Metal	Valence	Radius/Å	Me-O/F bond energy/(kJ·mol^{-1})	Crystal steady energy/(kJ·mol^{-1})
Li	+1	0.68	340.6/577.0	—
Mn	+3	0.62	402.0/423.4	150
Al	+3	0.50	512.1/663.6	—
Cr	+3	0.64	427.0/437.2	250.8
Co	+2	0.63	368.0/435.0	188.1
Mg	+2	0.65	393.7/461.9	—
O	-2	1.40	498.35/222.0	—
F	-1	1.36	—	—

Table 2 Capacities and cycle efficiency of $LiMn_{2-x}M_xO_{4-y}F_y$ (x=0.05; y=0.05; M= Al, Co, Cr, Mg)

Material	First			Tenth		Twentieth	
	Charge/ (mA·h·g^{-1})	Discharge/ (mA·h·g^{-1})	Efficiency/ %	Discharge/ (mA·h·g^{-1})	Efficiency/ %	Discharge/ (mA·h·g^{-1})	Efficiency/ %
$LiMn_2O_4$	133.51	122.04	91.41	115.80	94.89	112.27	91.99
$LiMnO_{4-y}F_y$	141.05	127.63	90.49	109.74	85.98	—	—
$LiMn_{2-x}Al_xO_{4-y}F_y$	131.99	124.59	94.40	117.31	94.16	118.07	94.77
$LiMn_{2-x}Co_xO_{4-y}F_y$	123.45	111.18	90.10	105.54	94.93	102.89	92.54
$LiMn_{2-x}Cr_xO_{4-y}F_y$	132.01	124.34	94.20	116.12	93.41	106.87	85.97
$LiMn_{2-x}Mg_xO_{4-y}F_y$	122.11	118.71	97.22	118.05	99.44	117.57	99.04

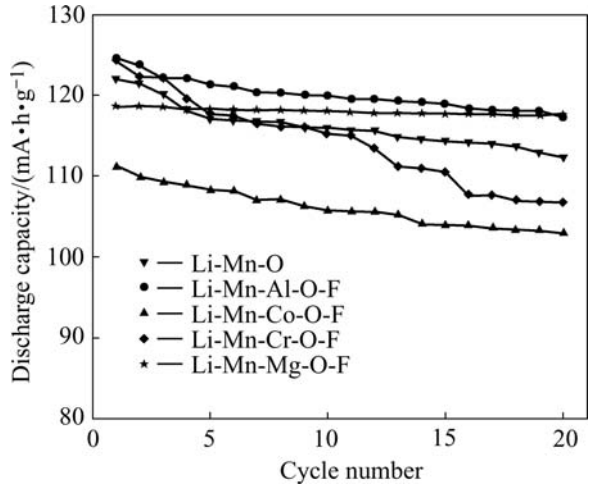

Fig.1 Cycle longevities curves of $LiMn_{2-x}M_xO_{4-y}F_y$ (x=0.05; y=0.05; M= Al, Co, Cr and Mg)

$O_{3.95}F_{0.05}$ during the twentieth charge-discharge process are respectively 94.77% and 99.04%, and the latter one has more promising trend of capacity retention.

Thus, it was thought that the performances of $LiMn_{2-x}M_xO_{4-y}F_y$ (x=0.05; y=0.05; M=Al and Mg) materials obviously preceded the pure $LiMn_2O_4$ material. So it is necessary to make further research on these two kinds of materials mentioned above from the angles of different synthesizing temperatures and reagents offering metal ions(Mg^{2+}), which would be described in the following contents.

3.2 Effects of different synthesizing temperature systems on performances of $LiMn_{2-x}Al_xO_{4-y}F_y$

The cycle performances of $LiMn_{2-x}Al_xO_{4-y}F_y$ (x=0.05; y=0.05) during 20 times charge-discharge process under different synthesizing temperatures are shown in Fig.2. It can be found that the electrochemical performances vary under different temperatures. At the temperature of 850 ℃, the performances of the material are the worst with the capacity of the first charge-discharge not reaching 110 mA·h/g and rapid fading, because spinel $LiMn_2O_4$, at such high temperature, suffers from severe loss of oxygen, which gives rise to impurity phases which, and then, affects the electrochemical performances of the material. Nevertheless, at the temperatures of 750 ℃ and 800 ℃, their performances are similar: the first capacity at 750 ℃ is slightly higher; the cycle longevity curve of this material at 800 ℃ is almost a beeline parallel to the x-axes and shows favorable cycle stability; after 20 times cycle processes, the capacities of the material at 750 ℃ and 800 ℃ correspond to each other.

Fig.3 shows the XRD patterns of $LiMn_{1.95}Al_{0.05}O_{3.95}F_{0.05}$ at the synthesizing temperature of 800 ℃, it can be seen that the diffraction maximum of the material is considerably acute and goes all the way with the criterion patterns. From this result, it can be estimated that $LiMn_{1.95}Al_{0.05}O_{3.95}F_{0.05}$ is the typical spinel material, whose position and intensity of characteristic absorption peak, compared with the XRD patterns of pure-phase $LiMn_2O_4$, are not evidently changed and whose half diffraction maximum is more narrow. This demonstrates that $LiMn_{1.95}Al_{0.05}O_{3.95}F_{0.05}$ has better crystallization capacity.

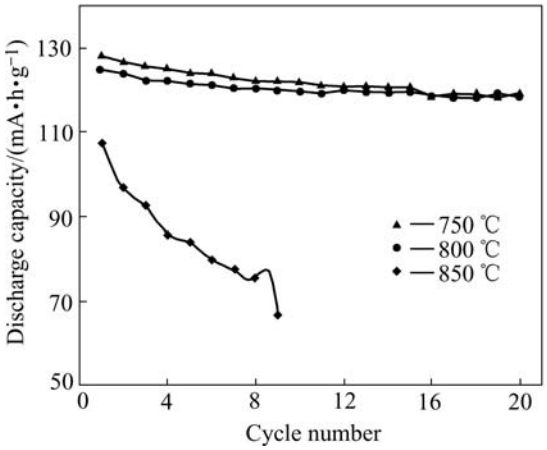

Fig.2 Cycle longevity curves of $LiMn_{0.95}Al_{0.05}O_{3.95}F_{0.05}$ at different temperatures

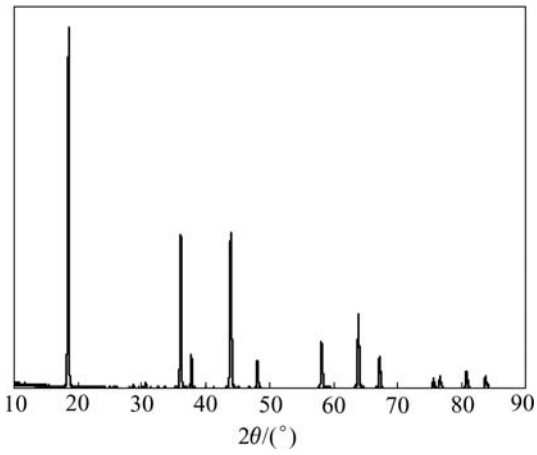

Fig.3 XRD patterns of $LiMn_{1.95}Al_{0.05}O_{3.95}F_{0.05}$ at synthesis temperature of 800 ℃

Fig.4 shows the SEM images of the $LiMn_{1.95}Al_{0.05}O_{3.95}F_{0.05}$ at the synthesizing temperature of 800 ℃. From these images, it can be found that the $LiMn_{1.95}Al_{0.05}O_{3.95}F_{0.05}$ maintains the favorable spinel octahedral structure with fine and uniform granularity around 0.8 μm and thus possesss relatively large active areas.

3.3 Effects of different reagents offering Mg ions on performances of $LiMn_{2-x}Mg_xO_{4-y}F_y$

When utilizing the method of high temperature solid-state reaction, there were two choices for the raw

materials: one reagent was MgF_2 which could offer both Mg and F to synthesize the cathode material of $LiMn_{2-x}Mg_xO_{4-y}F_y$(x=0.05; y=0.05); the other was $Mg(OH)_2$ and LiF which could respectively offer Mg and F to synthesize the cathode material of $LiMn_{2-x}Mg_xO_{4-y}F_y$(x=0.1; y=0.05).

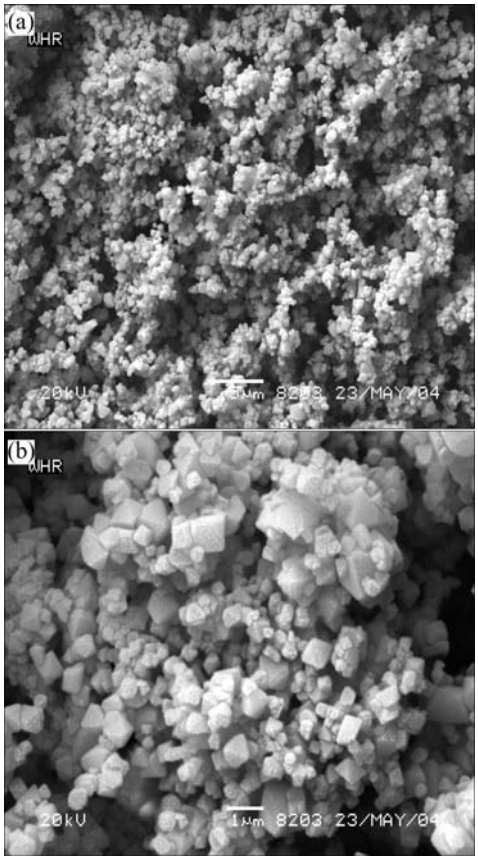

Fig.4 SEM images of $LiMn_{1.95}Al_{0.05}O_{3.95}F_{0.05}$ at synthesis temperature of 800 ℃: (a) 3 000 times; (b) 10 000 times

The curves of cycle performances of the $LiMn_{2-x}Mg_xO_{4-y}F_y$ are depicted in Fig.5, where Li-Mn-Mg-O-F(1) and Li-Mn-Mg-O-F(2) respectively represent $LiMn_{1.95}Mg_{0.05}O_{3.95}F_{0.05}$ and $LiMn_{1.90}Mg_{0.10}O_{3.95}F_{0.05}$ which were synthesized with $Mg(OH)_2$ and LiF as reagents, while Li-Mn-Mg-O-F(3) and Li-Mn-Mg-O-F(4) respectively represented $LiMn_{1.95}Mg_{0.05}O_{3.95}F_{0.05}$ and $LiMn_{1.90}Mg_{0.10}O_{3.95}F_{0.05}$ synthesized with only MgF_2 as reagent. It can be found from Fig.5, that Li-Mn-Mg-O-F(1) possesses not only higher capacity, but better cycle stability. Therefore, $LiMn_{1.95}Mg_{0.05}O_{3.95}F_{0.05}$, synthesized with $Mg(OH)_2$ and LiF as reagents is the best of all the materials of $LiMn_{2-x}Mg_xO_{4-y}F_y$(x=0.1; y=0.05).

Fig.6 shows the SEM images of the material of $LiMn_{1.95}Mg_{0.05}O_{3.95}F_{0.05}$. From this, the integrate crystal shape, which presents polyhedron appearance with trenchant edges and corners and uniform granularity between 0.5 μm and 2 μm, is found.

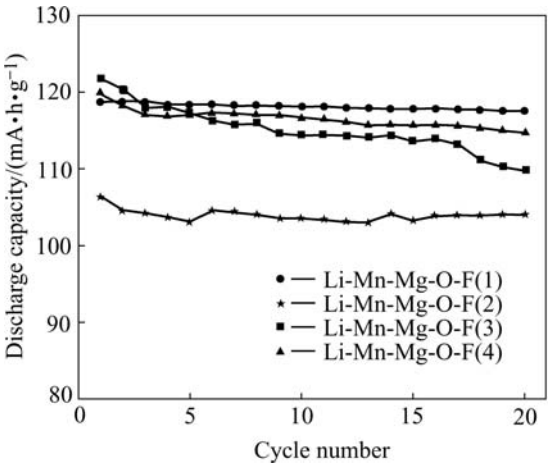

Fig.5 Curves of cycle performances of $LiMn_{2-x}Mg_xO_{4-y}F_y$ doped with Mg^{2+} offered by different reagents

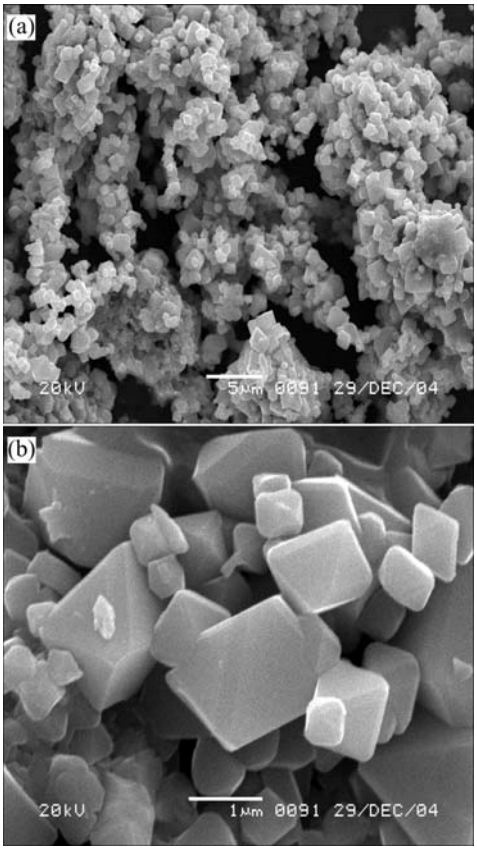

Fig.6 SEM images of material of $LiMn_{1.95}Mg_{0.05}O_{3.95}F_{0.05}$: (a) 3 000 times; (b) 20 000 times

3.4 Cyclic voltammetry tests of $LiMn_2O_4$ material co-doped with anti-electricity ions

The first cyclic voltammograms of the $LiMn_{1.95}Al_{0.05}O_{3.95}F_{0.05}$ material between 3.6 V and 4.5 V are recorded with the scan speed of 0.02 mV/s in Fig.7(b), where it can be found that the graph of $LiMn_{1.95}Al_{0.05}O_{3.95}F_{0.05}$, which presents two couples of redox peaks, is similar to that of spinel $LiMn_2O_4$, and the redox peaks of $LiMn_{0.95}Al_{0.05}O_{3.95}F_{0.05}$ are slightly wider

and the peak current is to some extent enhanced. In addition, the discrepancies of corresponding redox peaks of pure spinel $LiMn_2O_4$ are respectively 0.11 V and 0.1 V, and those of the materials co-doped are respectively 0.06 V and 0.07 V. The latter ones are obviously close to 0.058/n (n=1), which indicate that the reversibility of the electrode in embedding-doffing lithium is improved, and also explains the reasons why spinel $LiMn_2O_4$ co-doped possessed better cycle performance.

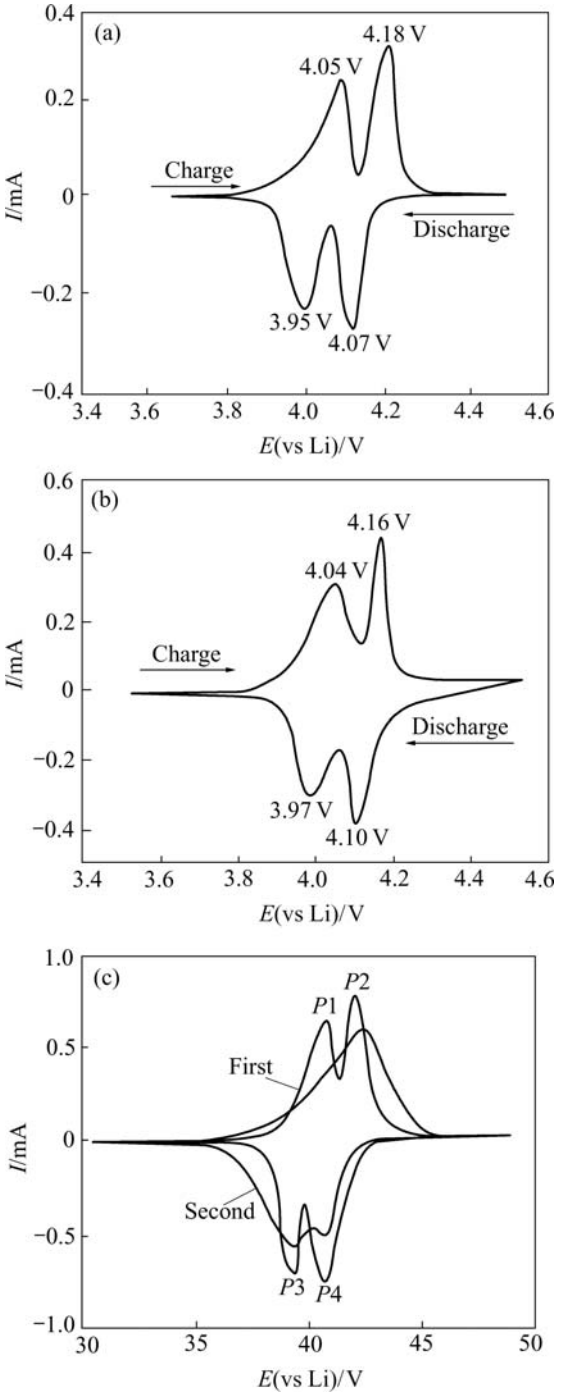

Fig.7 Cyclic voltammograms of spinel $LiMn_2O_4$ and that after co-doped: (a) Pure-phase Li-Mn-O; (b) $LiMn_{1.95}Al_{0.05}O_{3.95}F_{0.05}$; (c) $LiMn_{1.95}Mg_{0.05}O_{3.95}F_{0.05}$

The first and second cyclic voltammograms of the material of $LiMn_{1.95}Al_{0.05}O_{3.95}F_{0.05}$ between 3.6 V and 4.5 V are recorded with the scan speed of 0.02 mV/s in Fig.7(c), where it can be found that the graph of $LiMn_{1.95}Al_{0.05}O_{3.95}F_{0.05}$, which is similar to that of $LiMn_{1.95}Al_{0.05}O_{3.95}F_{0.05}$, also presents two couples of redox peaks, but the peak current is slightly higher. The two peaks, from the second cyclic voltammogram, show the trend of gradually combination during the embedding-doffing lithium process. This is due to the increasing times of cycling, which can hinder the process of embedding-doffing lithium and contributed to such trend in the cyclic voltammogram.

4 Conclusions

Four metal ions of Co^{3+}, Cr^{3+}, Al^{3+} and Mg^{2+} and the anion (F^-) were selected to improve the performances of $LiMn_2O_4$ by the method of anti-electricity co-doping. The results indicate that more prominent properties are possessed by the $LiMn_{1.95}Al_{0.05}O_{3.95}F_{0.05}$ and the $LiMn_{1.95}Mg_{0.05}O_{3.95}F_{0.05}$, whose reversible capacities, after 20 times cycle process, maintain 118.07 mA·h/g and 117.57 mA·h/g respectively and the efficiencies of the capacity retention are 94.77% and 99.04%, respectively. These data show their better electrochemical performances than those of pure-phase $LiMn_2O_4$.

The research on the effects of different sintering temperature on the material of $LiMn_{1.95}Al_{0.05}O_{3.95}F_{0.05}$ indicates that the material, at the temperature of 800 ℃, presents the integrate crystal shape and favorable cycle performance; the research on the effects of different reagents offering Mg doped into $LiMn_2O_4$ on the properties of $LiMn_{2-x}Mg_xO_{4-y}F_y$ shows that $LiMn_{1.95}Mg_{0.05}O_{3.95}F_{0.05}$ synthesized with $Mg(OH)_2$ and LiF as the reagents respectively offering Mg and F is the best of all materials of this kind due to its integrate crystal structure and stability capacity.

The results of cyclic voltammetry test indicate that $LiMn_2O_4$ possesses two obvious couples of redox peaks, and after co-doped with anti-electricity ions, the shape of such peaks of the material is more integrate and symmetrical. This shows that the materials co-doped possess preferable electrochemical reversibility.

References

[1] ZHONG Hui, XU Hui. Preparation and electrochemical properties of $LiCo_{0.3}Ni_{0.7-x}Sr_xO_{0.2}$ cathode material for lithium ion batteries[J]. The Chinese Journal of Nonferrous Metals, 2004, 14(2): 157−161.(in Chinese)

[2] TANG Hong-wei, CHEN Zong-zhang, ZHONG Fa-ping. Synthesis and electrochemical behavior of $LiNi_{1-x}M_xO_2$(M=Co^{3+}, Al^{3+})[J]. The Chinese Journal of Nonferrous Metals, 2003, 13(4): 859−863.(in Chinese)

[3] LI Hui, ZHAI Yu-chun, TIAN Yan-wen. Preparation and properties of $LiNi_{1-y}Al_yO_2$ as cathodematerial in lithium ion battery[J]. The Chinese Journal of Nonferrous Metals, 2003, 13(3): 690−694.(in Chinese)

[4] WANG Zhi-xing, ZHANG Bao, LI Xin-hai, et al. Synthesis and performance of lithium rich spinels $Li_{1+x}Mn_{2-x}O_4$[J]. The Chinese Journal of Nonferrous Metals, 2004, 14(9): 1525−1529.(in Chinese)

[5] CHEN Y, WANG G X, KONSTANTINOV K, LIU H K, DOU S X. Synthesis and characterization of $LiCo_xMn_yNi_{1-x-y}O_2$ as a cathode material for secondary lithium batteries[J]. J Power Source, 2003, 119-121: 184−188.

[6] PARK Y J, HONG Y S, WU X L, RYU K S, CHANG S H. Synthesis and electrochemical characteristics of $Li[Co_xLi_{(1/3-x/3)}Mn_{(2/3-2x/3)}]O_2$ Compounds[J]. J Power Source, 2004(129): 288−295.

[7] HWANG B J, SANTHANAM R, HU S G. Synthesis and characterization of multidoped lithium manganese oxide spinel, $Li_{1.02}Co_{0.1}Mn_{1.8}O_4$ for rechangeable lithium batteries[J]. J Power Source, 2002(108): 250−255.

[8] WANG G X, BEWLAY S, YAO J, CHEN Y, GUO Z P, LIU H K, DOU S X. Multiple-ion-doped lithium nickel oxide as cathode materials for lithium-ion batteries[J]. J Power Source, 2003(119): 189−194.

[9] ROBERSTON A D, AREMSTRONG A R, BRUCE P G. Low temperature lithium manganese cobalt oxide spinels, $Li_{4-x}Mn_{5-2x}Co_{3x}O_{12}(0 \leqslant x \leqslant 1)$, for use as cathode materials in rechangeable lithium batteries[J]. J Power Source, 2001(97): 332−335.

[10] ZHANG Bao, LUO Wen-bin, LI Xin-hai, WANG Zhi-xing. Electrochemical properties of $LiFePO_4$/C for cathode materials of lithium ion batteries[J]. The Chinese of Journal of Nonferrous Metals, 2005, 15(2): 300−304.(in Chinese)

[11] LIU Zhao-lin, WANG Hong-bin, FANG Ling. Improving the high-temperature perfomance of $LiMn_2O_4$ spinel by micro-emulsion coating of $LiCoO_2$[J]. J Power Sources, 2002(104): 101−107.

[12] LI Zhi-guang, LIU Su-qin, HUANG Ke-long. Synthesis of spinel typed $LiMn_2O_4$ and its properties[J]. The Chinese Journal of Nonferrous Metals, 2003, 13(2): 526−529.(in Chinese)

[13] YU Xiao-yuang, HU Guo-rong, XIAO Jin, PENG Zhong-dong, LIU Ye-xiang. Surface modification of $LiCo_{0.05}Mn_{1.95}O_4$ cathode by coating with SiO_2-TiO_2 composite[J]. The Chinese Journal of Nonferrous Metals, 2004, 14(4): 723.(in Chinese)

[14] CHEN Zhao-Yong, HE Yi, LI Zhi-Jie. Synthesis and electrochemical performance of spinel $LiMn_2O_{4-x}(SO_4)_x$ cathode materials[J]. Chinese Journal Chemistry, 2002, 20: 194−197.

[15] CHEN Zhao-yong, ZHU Hua-li, HU Guo-rong, LIU Ye-xiang. Electrochemical performance and structure characteristic of $LiMn_2O_{4-x}Y_x$(Y=F, Cl, Br) compounds[J]. Trans Nonferrous Met Soc China, 2004, 14(6): 1151−1155.

(Edited by LI Xiang-qun)